



Title	Cationic ring-opening copolymerization of a cyclic acetal and $\gamma$ -butyrolactone: monomer sequence transformation and polymerization-depolymerization control by vacuuming or temperature changes
Author(s)	Takebayashi, Kana; Kanazawa, Arihiro; Aoshima, Sadahito
Citation	Polymer Journal. 2023, 56, p. 309-317
Version Type	VoR
URL	<a href="https://hdl.handle.net/11094/93299">https://hdl.handle.net/11094/93299</a>
rights	This article is licensed under a Creative Commons Attribution 4.0 International License.
Note	

*The University of Osaka Institutional Knowledge Archive : OUKA*

<https://ir.library.osaka-u.ac.jp/>

The University of Osaka



# Cationic ring-opening copolymerization of a cyclic acetal and $\gamma$ -butyrolactone: monomer sequence transformation and polymerization–depolymerization control by vacuuming or temperature changes

Kana Takebayashi<sup>1</sup> · Arihiro Kanazawa <sup>1</sup> · Sadahito Aoshima<sup>1</sup>

Received: 6 September 2023 / Revised: 2 October 2023 / Accepted: 2 October 2023  
© The Author(s) 2023. This article is published with open access

## Abstract

Polymerization–depolymerization equilibrium is a promising strategy for the construction of polymerization systems through which sustainable polymers can undergo reversible polymer–monomer transformations. In this study, we perform monomer sequence transformation and copolymer depolymerization, which are based on transacetalization reactions and polymerization–depolymerization equilibrium, in the cationic ring-opening copolymerization of 2-methyl-1,3-dioxepane and  $\gamma$ -butyrolactone with a protonic acid. The removal of monomer molecules from the copolymerization solution by vacuuming with a vacuum pump caused monomer sequence to transform into pseudo-alternating copolymer chains and subsequently depolymerize into oligomers. Increasing the temperature during copolymerization also resulted in depolymerization, while copolymers were regenerated by the subsequent decrease in temperature.

## Introduction

Recently, emerging demands for polymers with low environmental loads have shed light on recyclable polymers and degradable polymers. One ideal polymer recycling or degradation method is to produce original monomers from polymers by depolymerization. A polymerization–depolymerization equilibrium primarily relies on the Gibbs free energy of propagation reactions; hence, to achieve efficient and smooth depolymerization into monomers, it is essential to fine tune the energy balance by designing monomers and reaction conditions. Conventional studies on depolymerization reactions have often focused on the polymerization–depolymerization

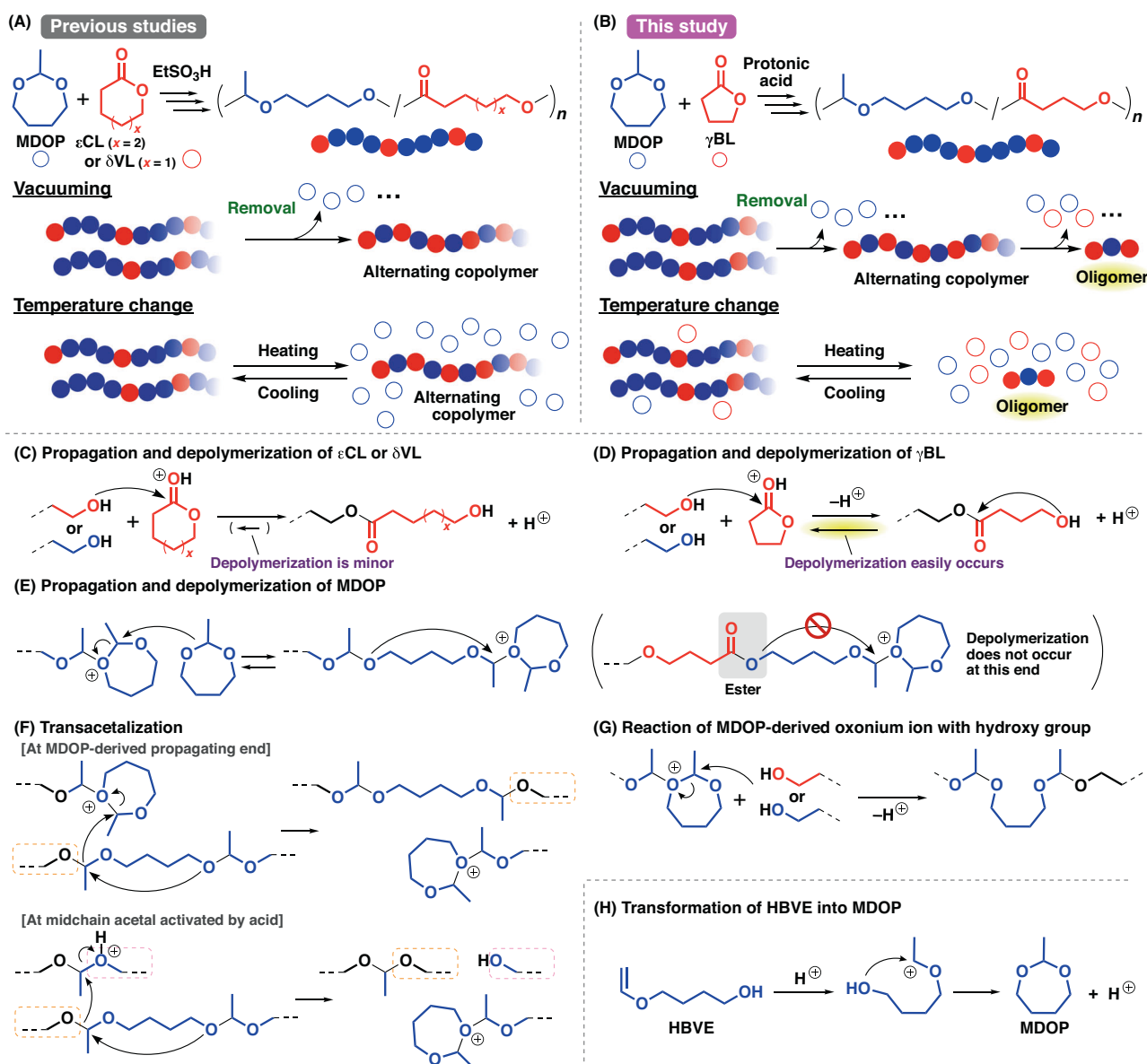
equilibrium based on the equilibrium monomer concentration, which is also related to the ceiling temperature ( $T_c$ ); in contrast, recent studies purposefully employ depolymerization reactions to develop recyclable polymers that undergo closed-loop chemical recycling [1–4].

Monomer sequences in polymer chains can also be controlled when polymerization–depolymerization equilibria are employed in copolymerization. The cationic polymerizations of cyclic acetals [5–7] and cyclic esters [8–11] by a protonic acid catalyst involve a polymerization–depolymerization equilibrium, particularly when monomers with low homopolymerizability (i.e., high equilibrium monomer concentrations) are used. In our previous study on the cationic copolymerizations of 2-methyl-1,3-dioxepane (MDOP) and  $\epsilon$ -caprolactone ( $\epsilon$ CL), copolymers that contain isolated single  $\epsilon$ CL units among MDOP blocks were transformed into alternating copolymers by removing MDOP monomers from a reaction solution by vacuuming (Scheme 1A) [12]. This monomer sequence transformation occurred because the depolymerization of MDOP was promoted in the polymerization–depolymerization equilibrium by the removal of MDOP (Scheme 1E). Transacetalization reactions in polymer chains are also important for the transfer of midchain MDOP homosequences into chain end

**Supplementary information** The online version contains supplementary material available at <https://doi.org/10.1038/s41428-023-00847-9>.

- ✉ Arihiro Kanazawa  
kanazawaal1@chem.sci.osaka-u.ac.jp
- ✉ Sadahito Aoshima  
aoshima@chem.sci.osaka-u.ac.jp

<sup>1</sup> Department of Macromolecular Science, Graduate School of Science, Osaka University, Toyonaka, Osaka 560-0043, Japan



**Scheme 1** Schematic illustrations of (A) previous studies and (B) this study. (C)–(G) Reactions that occur in the copolymerization of MDOP and cyclic esters. (H) In situ generation of MDOP from HBVE

locations at which depolymerization occurs (Scheme 1F). Monomer sequence transformation was also demonstrated to occur, which is achieved by controlling the polymerization–depolymerization equilibrium via temperature change, in the cationic copolymerizations of MDOP and  $\epsilon$ CL or  $\delta$ -valerolactone ( $\delta$ VL) [13]. In these previous studies, further depolymerization reactions from the alternating chains did not occur because  $\epsilon$ CL- and  $\delta$ VL-derived units were inert (Scheme 1C) at room temperature due to the low equilibrium monomer concentrations (i.e., the high  $T_c$ s;  $T_c$  of 261 °C [ $\epsilon$ CL] and 155 °C [ $\delta$ VL] for an equilibrium monomer concentration of 1 M [14]).

In this study, we focused on  $\gamma$ -butyrolactone ( $\gamma$ BL) as a comonomer for cationic copolymerization with MDOP (Scheme 1B).  $\gamma$ BL has been regarded as a non-homopolymerizable monomer due to the high equilibrium monomer concentration (i.e., the low  $T_c$ ;  $T_c$  of –131 °C for an equilibrium monomer concentration of 1 M [14]), while  $\gamma$ BL homopolymerization was attained by the development of effective catalysts several years ago [15–19]. Chemical recycling of poly( $\gamma$ BL) into a  $\gamma$ BL monomer was also achieved by smooth depolymerization. The low homopolymerizability of  $\gamma$ BL is very attractive for the control of polymerization–depolymerization (Scheme 1D) in not only homopolymerization but also copolymerization. As explained

above,  $\epsilon$ CL and  $\delta$ VL-derived ends negligibly underwent depolymerization (Scheme 1C) in the copolymerization with MDOP. In contrast, based on investigations with  $\gamma$ BL in this study, monomer sequences were transformed into pseudo-alternating sequences and subsequently degraded into oligomers through controlling polymerization–depolymerization equilibria, which was achieved by removing monomers through vacuuming or by temperature changes.

## Experimental section

### Materials

4-Hydroxybutyl vinyl ether (HBVE; Sigma-Aldrich, >99%) and  $\gamma$ BL (TCI, >99.0%) were distilled twice from calcium hydride under reduced pressure. EtSO<sub>3</sub>H (Sigma-Aldrich, >95.0%), PhSO<sub>3</sub>H (TCI, >98.0%), 2,4,5-trichlorobenzenesulfonic acid (C<sub>6</sub>H<sub>2</sub>Cl<sub>3</sub>SO<sub>3</sub>H; TCI, >98.0%), benzyl alcohol (Kanto Chemical, >99.0%), and 1,5,7-triazabicyclo[4.4.0]dec-5-ene (TBD; Sigma-Aldrich, 98.0%) were used as received. Toluene (Wako, >99.5%) was dried by passage through solvent purification columns (Glass Contour).

### Polymerization procedure

A glass tube equipped with a three-way stopcock was dried using a heat gun (Ishizaki PJ-206A; the blowing temperature was ~450 °C) under a dry nitrogen atmosphere. Toluene, HBVE, and  $\gamma$ BL were sequentially added to the tube using dry syringes. Polymerization was initiated by adding a protonic acid solution in toluene. After predetermined intervals, aliquots were withdrawn from the reaction solution using dry syringes and subsequently added to vials containing methanol and a small amount of aqueous ammonia. The quenched mixtures were diluted with dichloromethane and washed with water. The volatile materials were removed under reduced pressure at 50 °C to afford polymers. Monomer conversion was calculated from the <sup>1</sup>H NMR spectra of the quenched reaction mixtures. The polymer yield was not determined. Vacuuming during polymerization was conducted with a vacuum pump (SATO VAC TSW-50). The pressure was ~5 mmHg.

### Characterization

The molecular weight distribution (MWD) of the polymers was measured by gel permeation chromatography (GPC) in chloroform at 40 °C with polystyrene gel columns [TSKgel GMH<sub>HR</sub>-M $\times$ 2 (exclusion limit MW = 4  $\times$  10<sup>6</sup>; bead size = 5  $\mu$ m; column size = 7.8 mm i.d.  $\times$  300 mm); flow rate = 1.0 ml/min] connected to a JASCO PU-4580 pump, a

Tosoh CO-8020 column oven, a Tosoh UV-8020 ultraviolet detector, and a Tosoh RI-8020 refractive-index detector. The number-average molecular weight ( $M_n$ ) and the polydispersity ratio (weight-average molecular weight/number-average molecular weight [ $M_w/M_n$ ]) were calculated from the chromatographs based on 16 polystyrene standards (Tosoh;  $M_n$  = 5.0  $\times$  10<sup>2</sup>–1.09  $\times$  10<sup>6</sup>,  $M_w/M_n$  < 1.2). NMR spectra were recorded by a JEOL JNM-ECA 500 spectrometer (500.16 MHz for <sup>1</sup>H and 125.77 MHz for <sup>13</sup>C) or a JEOL JNM-ECA 400 spectrometer (399.78 MHz for <sup>1</sup>H and 100.53 MHz for <sup>13</sup>C) in chloroform-*d* at 30 °C. Electrospray ionization mass spectrometry (ESI-MS) data were acquired on an LTQ Orbitrap XL (Thermo Scientific) spectrometer.

### Transesterification

A polymer was dissolved in butyl acetate. Transesterification was started by adding a Ti(OBu)<sub>4</sub> solution. After the reaction was performed at 70 °C for 21.5 h, the solution was diluted with dichloromethane at room temperature to quench the reaction. The quenched solution was washed with water, and volatile materials were removed under reduced pressure at 60 °C to yield a product.

## Results and discussion

### Investigation on the suitable reaction conditions for cationic copolymerization of MDOP and $\gamma$ BL

To determine the appropriate reaction conditions, cationic copolymerizations of a cyclic acetal MDOP and a cyclic ester  $\gamma$ BL were conducted at different monomer concentrations and protonic acid catalysts. MDOP was used as a cyclic acetal monomer because this monomer was suitable for copolymerizations with  $\epsilon$ CL and  $\delta$ VL [12, 13]. MDOP was synthesized in situ from HBVE in a polymerization solution as performed in our previous studies (Scheme 1H) [12, 13]. The concentrations of MDOP and  $\gamma$ BL greatly impacted the occurrence of polymerization. Both monomers were not consumed at MDOP/ $\gamma$ BL concentrations of 0.50 M/0.50 M in the reaction with EtSO<sub>3</sub>H as a catalyst (entry 1 in Table 1). The increase in the MDOP concentration to 2.5 M resulted in the consumption of both monomers (entry 2); however, the product was an oligomer with an  $M_n$  value of 0.8  $\times$  10<sup>3</sup>. Interestingly, when the  $\gamma$ BL concentration was also increased from 0.50 M to 2.0 M, a polymer with a bimodal MWD containing a portion of molecular weights (MWs) greater than 10<sup>4</sup> was obtained (entry 3; Fig. 1A). The  $M_n$  value of the higher-MW peak was 10  $\times$  10<sup>3</sup>. Ineffective copolymerizations at low concentrations of MDOP and/or  $\gamma$ BL (entries 1 and 2) probably result from the low homopolymerizability of not only  $\gamma$ BL but also MDOP. MDOP was reported to have

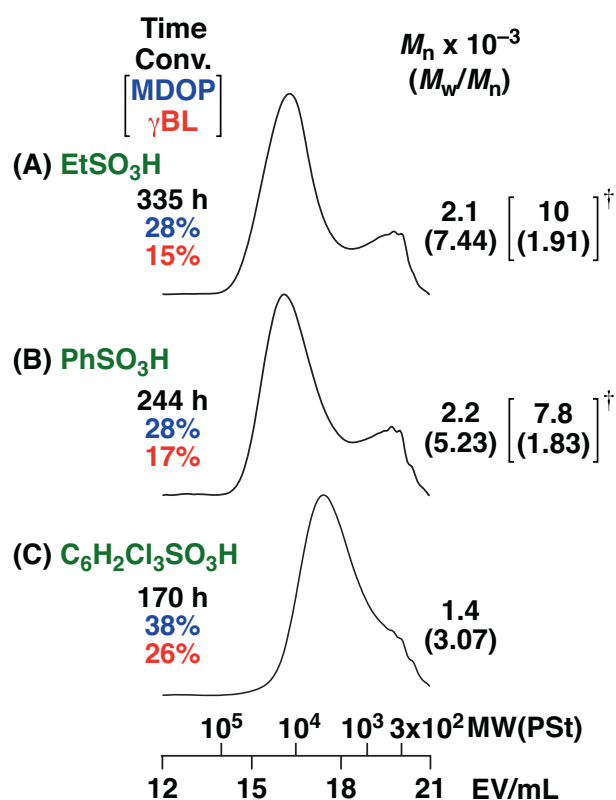
**Table 1** Cationic copolymerization of MDOP and  $\gamma$ BL<sup>a</sup>

Entry	Conc (M)		Catalyst	Time	Conv (%) <sup>c</sup>		$M_n \times 10^{-3}^d$	$M_w/M_n^d$	Units per block <sup>e</sup>	
	MDOP <sup>b</sup>	$\gamma$ BL			MDOP	$\gamma$ BL			MDOP	$\gamma$ BL
1	0.50	0.50	EtSO <sub>3</sub> H	143 h	0	0	—	—	—	—
2	2.5	0.50	EtSO <sub>3</sub> H	119 h	8	9	0.8	2.91	4.6	1.1
3	2.5	2.0	EtSO <sub>3</sub> H	335 h	28	15	2.1 [10] <sup>f</sup>	7.44	2.5	1.2
4	2.5	2.0	PhSO <sub>3</sub> H	244 h	28	17	2.2 [7.8] <sup>f</sup>	5.23	2.5	1.2
5	2.5	2.0	C <sub>6</sub> H <sub>2</sub> Cl <sub>3</sub> SO <sub>3</sub> H	170 h	38	26	1.4	3.07	2.3	1.2
6	2.5	4.0	EtSO <sub>3</sub> H	336 h	43	18	3.2 [8.0] <sup>f</sup>	4.56	1.8	1.3
7	5.0	2.0	EtSO <sub>3</sub> H	270 h	59	43	6.2 [19] <sup>f</sup>	6.15	3.1	1.1
8	—	5.0	EtSO <sub>3</sub> H	216 h	—	0	—	—	—	—

<sup>a</sup>[Catalyst]<sub>0</sub> = 4.0 mM, in toluene at 30 °C<sup>b</sup>Synthesized from HBVE in situ (Scheme 1H)<sup>c</sup>Determined by <sup>1</sup>H NMR<sup>d</sup>Determined by GPC (polystyrene calibration)<sup>e</sup>By <sup>1</sup>H NMR<sup>f</sup>Values for the main peak

an equilibrium monomer concentration ( $[MDOP]_e$ ) of 2.7 M at 30 °C (this corresponds to a  $T_c$  of  $-37$  °C for an equilibrium monomer concentration of 1 M) [20]. The increase in the  $\gamma$ BL concentration resulted in effective copolymerization (entry 3) via the promoted reactions between MDOP and  $\gamma$ BL (Monomer reactivity ratios are useful for discussing copolymerization behavior. However, it is unclear whether monomer reactivity ratios can be determined for the copolymerization that involves intra- and intermolecular transacetalization reactions).

<sup>1</sup>H NMR analysis of the obtained polymer (Fig. 2A) indicated that the structures of the polymer chains result from the reactions between MDOP and  $\gamma$ BL. A spectrum of a  $\gamma$ BL homopolymer, which was produced by a strong organobase catalyst (TBD) [18], is also shown in Fig. 2B for comparison. An obvious difference between the two spectra is the peak for the methylene group at the center of the propylene unit derived from  $\gamma$ BL at 1.8–2.0 ppm (peaks 8 and 13). The methylene peak in the  $\gamma$ BL homosequences was observed at 1.96 ppm (peak 13) in Fig. 2B, while this peak was very small in the copolymer spectrum (Fig. 2A), indicating that  $\gamma$ BL homosequences were not efficiently generated during copolymerization with MDOP. The methylene peak of a  $\gamma$ BL unit located between MDOP units was present at a higher field (1.88 ppm, peak 8) than the corresponding methylene peak in  $\gamma$ BL homosequences. The other two methylene groups of the propylene unit derived from  $\gamma$ BL exhibited peaks in similar regions in both spectra, although the oxygen-adjacent methylene peak ( $\sim 4.1$  ppm) was observed at a slightly higher field in the copolymer spectrum (peak 6) than in the homopolymer spectrum (peak 14). Based on the integral ratios of these peaks and the peaks assigned to

**Fig. 1** MWD curves of the MDOP- $\gamma$ BL copolymers. Entries (A) 3, (B) 4, and (C) 5 in Table 1. <sup>†</sup>Values for the main peak

MDOP units, the average number of MDOP/ $\gamma$ BL units per block was calculated to be 2.5/1.2.

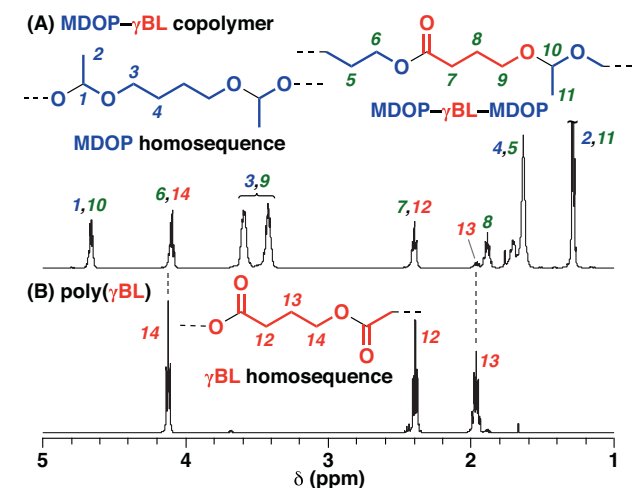
The initial monomer concentrations affected the average number of monomer units per block and MWs. A further increase in the initial concentration of  $\gamma$ BL to 4.0 M resulted

in a copolymer with 1.8/1.3 MDOP/ $\gamma$ BL units (entry 6; see Fig. S1 for the  $^{13}\text{C}$  NMR spectrum of this polymer). Analyses of the copolymers obtained at different reaction times indicated that the length of the MDOP blocks gradually decreased as the copolymerization proceeded (Figs. S2–S4; entries 3, 6, and 7). In addition, very long MDOP homosequences were generated in the very early stage of the copolymerizations, while considerable amounts of the MDOP homosequences were smoothly transformed into

MDOP monomers (Figs. S2 and S4). A polymer with a high MW was obtained at MDOP and  $\gamma$ BL concentrations of 5.0 M and 2.0 M, respectively (entry 7). The  $M_n$  value of the main peak was  $19 \times 10^3$ . Homopolymerization of  $\gamma$ BL did not proceed with  $\text{EtSO}_3\text{H}$  as a catalyst (entry 8), which is consistent with the inefficient generation of  $\gamma$ BL homosequences in the copolymerization.

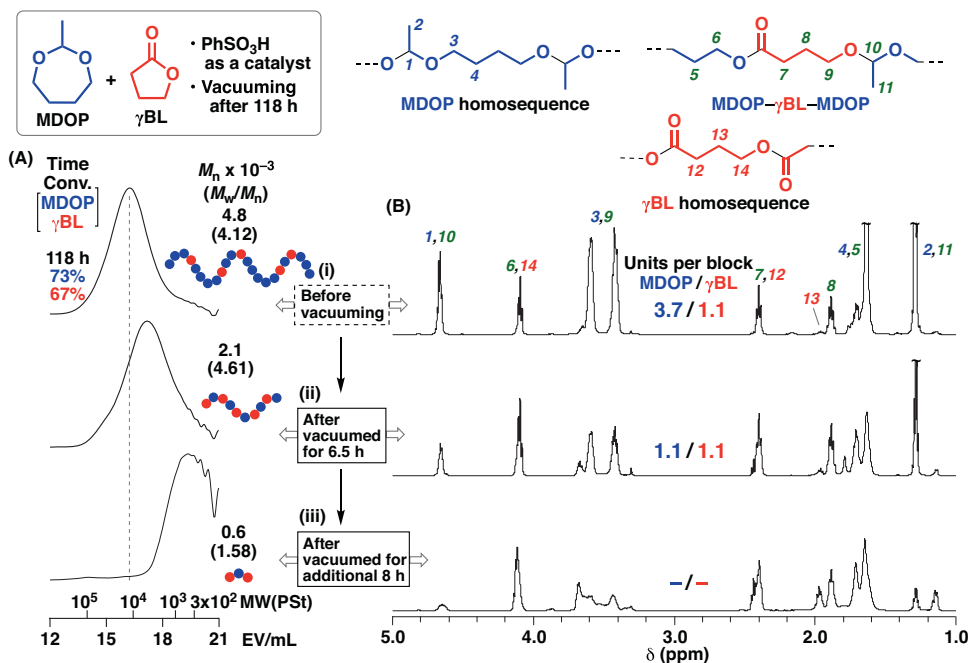
ESI-MS analysis of a copolymer suggested that a low-MW peak of the bimodal MWD mainly consists of cyclic chains. The ESI-MS spectrum of the copolymer obtained above (entry 6 in Table 1; see Fig. S5A for the MWD curve) exhibited main peaks with  $m/z$  values that are consistent with the values of cyclic chains in the low-MW region (Fig. S5B). It is unclear whether linear or cyclic chains are mainly contained in the high-MW peak of the bimodal MWD because high-MW compounds were not sufficiently detected in ESI-MS analysis.

The effects of protonic acid catalysts were also examined using  $\text{PhSO}_3\text{H}$  and 2,4,5-trichlorobenzenesulfonic acid ( $\text{C}_6\text{H}_2\text{Cl}_3\text{SO}_3\text{H}$ ). The acidity increases in the order of  $\text{EtSO}_3\text{H} < \text{PhSO}_3\text{H} < \text{C}_6\text{H}_2\text{Cl}_3\text{SO}_3\text{H}$  [21] (the acidity order of  $\text{C}_6\text{H}_2\text{Cl}_3\text{SO}_3\text{H}$  was not reported; however, this acid is most likely stronger than  $\text{PhSO}_3\text{H}$  due to the three chlorine atoms). Copolymerization using  $\text{PhSO}_3\text{H}$  yielded a product with a similar MW to that obtained with  $\text{EtSO}_3\text{H}$  (entry 4 in Table 1 and Fig. 1B). In contrast, utilizing  $\text{C}_6\text{H}_2\text{Cl}_3\text{SO}_3\text{H}$  resulted in a lower-MW product (entry 5; Fig. 1C) compared to the above two cases. Based on these results, we used  $\text{EtSO}_3\text{H}$  or  $\text{PhSO}_3\text{H}$  as a catalyst in copolymerizations for monomer sequence transformation, as demonstrated below.

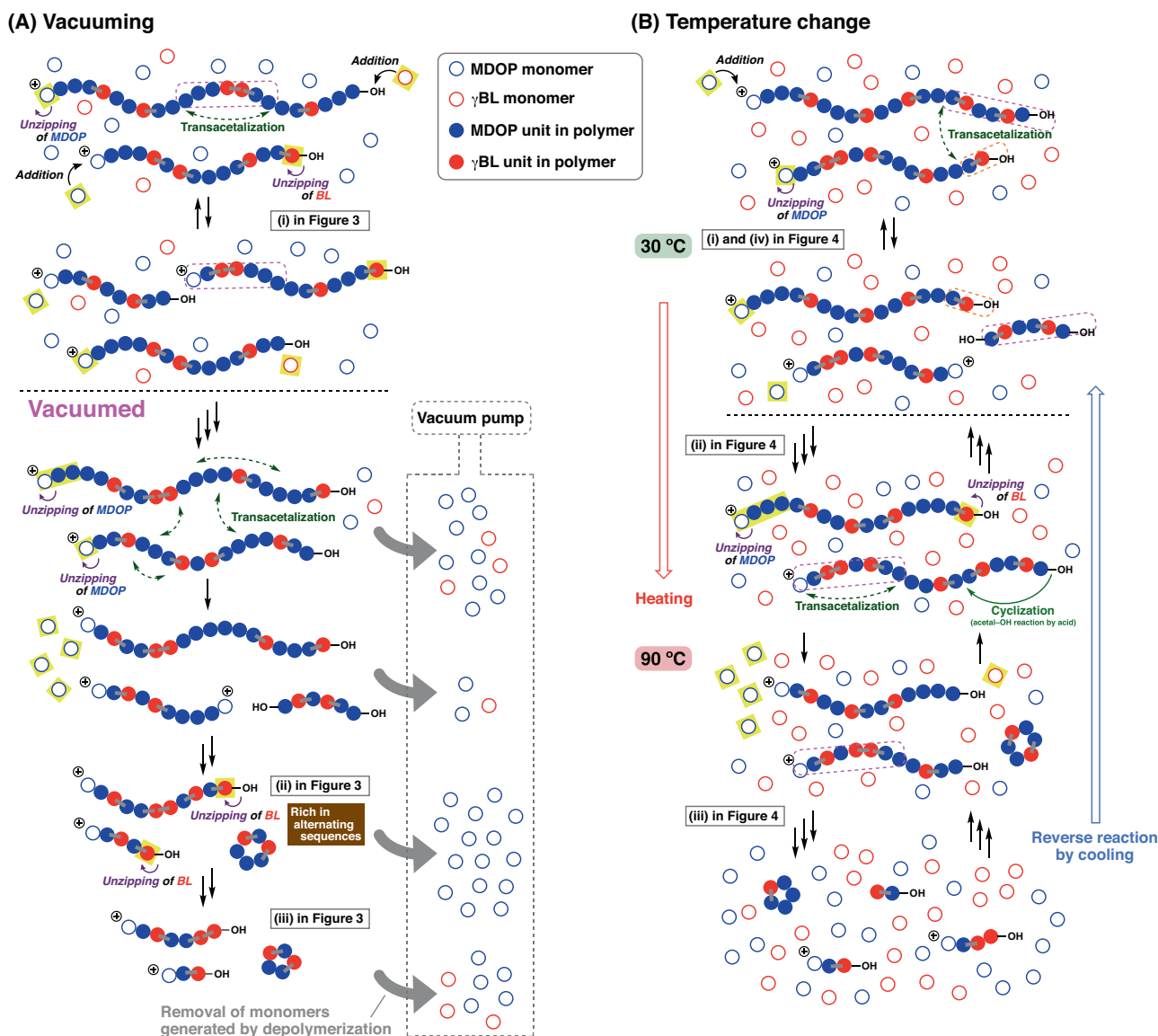


**Fig. 2**  $^1\text{H}$  NMR spectra of (A) the MDOP- $\gamma$ BL copolymer (entry 3 in Table 1) and (B) the  $\gamma$ BL homopolymer ( $[\gamma\text{BL}]_0 = 9.5$  M,  $[\text{benzyl alcohol}]_0 = 19$  mM,  $[\text{TBD}]_0 = 9.5$  mM, in dichloromethane at  $-40^\circ\text{C}$ ; conv = 35% (24 h),  $M_n(\text{GPC}) = 1.6 \times 10^3$ ; the spectrum of the high-MW portion separated by preparative GPC). See Scheme S1 for other possible structures

**Fig. 3** (A) MWD curves and (B)  $^1\text{H}$  NMR spectra (in  $\text{CDCl}_3$  at  $30^\circ\text{C}$ ) of the poly(MDOP-co- $\gamma$ BL)s obtained (i) before and (ii), (iii) after vacuuming. Polymerization conditions:  $[\text{HBVE (MDOP)}]_0 = 6.6$  M,  $[\gamma\text{BL}]_0 = 2.1$  M,  $[\text{PhSO}_3\text{H}]_0 = 4.0$  mM, at  $30^\circ\text{C}$  (before vacuuming) or room temperature (after vacuuming). See Scheme S1 for other possible structures







**Scheme 2** Schematic illustration of (A) depolymerization by vacuuming and (B) depolymerization–polymerization control by temperature change. The  $\gamma$ BL-derived chain ends (red symbols with an

OH group) may be unstable due to the very low  $T_c$  of  $\gamma$ BL, although these chain ends can be transiently generated

### Monomer sequence control by vacuuming

As explained in the “Introduction” section, vacuuming during the copolymerization of MDOP and  $\gamma$ BL potentially results in transformation from MDOP homosequence-containing copolymers to alternating copolymers and further depolymerization into oligomeric products due to the high equilibrium concentration (low ceiling temperature) of  $\gamma$ BL [14]. To conduct this vacuuming experiment, a copolymer with MDOP homosequence blocks and isolated single  $\gamma$ BL units was prepared by copolymerization at MDOP/ $\gamma$ BL concentrations of 6.6 M/2.1 M with  $\text{PhSO}_3\text{H}$  as a catalyst. The copolymer obtained in 118 h has an  $M_n$  of  $4.8 \times 10^3$  (Fig. 3A, (i)), and the average number of MDOP/ $\gamma$ BL units

per block is 3.7/1.1 (Fig. 3B, (i)). Subsequently, the polymerization solution was vacuumed with a vacuum pump to remove MDOP and  $\gamma$ BL monomers. After vacuuming was performed for 6.5 h, the  $M_n$  value of the polymer decreased to  $2.1 \times 10^3$  (Fig. 3A, (ii)), suggesting that depolymerization partly occurred. The  $^1\text{H}$  NMR analysis revealed that the copolymer had almost alternating sequences at this stage (Scheme 2A), as demonstrated by the number of MDOP/ $\gamma$ BL units per block of 1.1/1.1 (Fig. 3B, (ii); see Fig. S6 for the degradation of an alternating copolymer (obtained at initial MDOP/ $\gamma$ BL concentrations of 2.5 M/2.0 M) by transesterification). A possible mechanism that explains the transformation from MDOP homosequence-containing copolymers into alternating copolymers is as follows [12]: removing

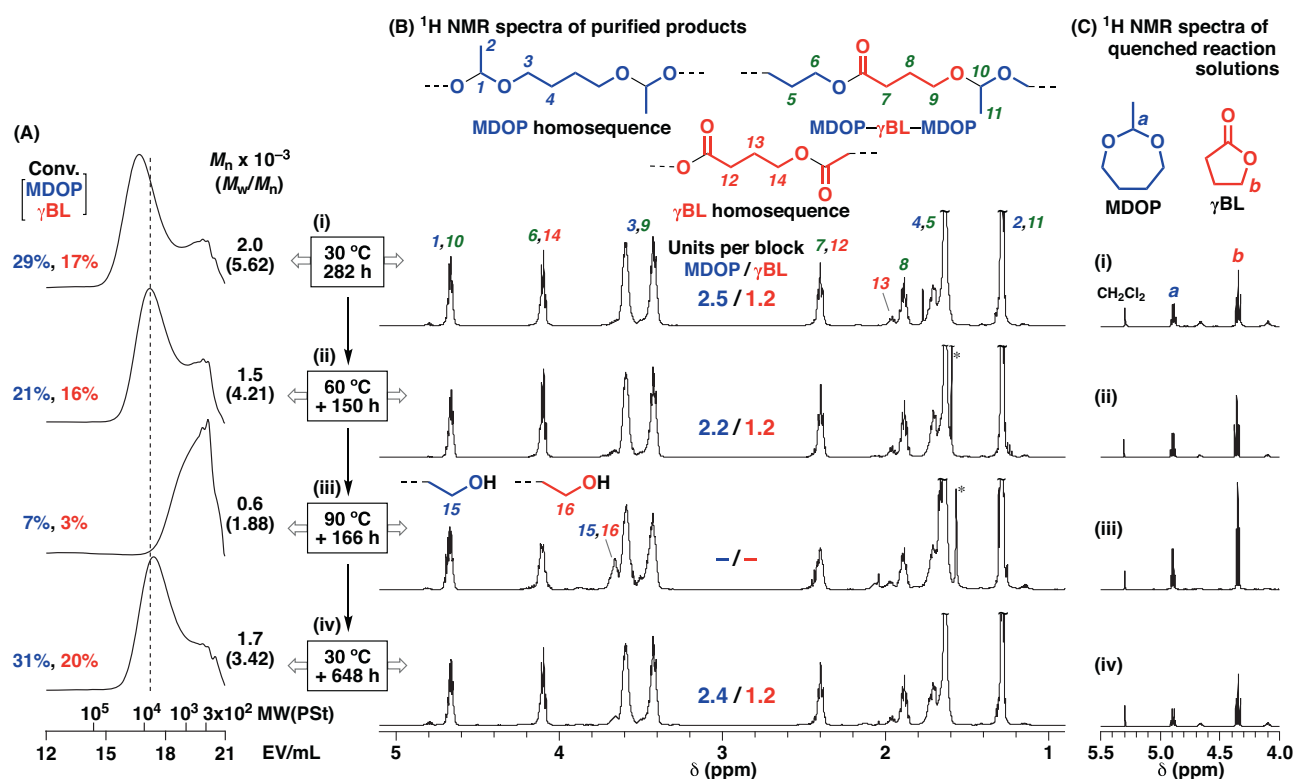


**Fig. 4** (A) MWD curves and (B)  $^1\text{H}$  NMR spectra (in  $\text{CDCl}_3$  at 30 °C) of the poly(MDOP-co- $\gamma$ BL)s. Polymerization conditions (the same conditions as those for entry 4 in Table 1 except for temperature change):  $[\text{HBVE}(\text{MDOP})]_0 = 2.5 \text{ M}$ ,  $[\gamma\text{BL}]_0 = 2.0 \text{ M}$ ,  $[\text{PhSO}_3\text{H}]_0 =$

4.0 mM, in toluene at (i) 30 → (ii) 60 → (iii) 90 → (iv) 30 °C. (C)  $^1\text{H}$  NMR spectra (in  $\text{CDCl}_3$  at 30 °C) of the quenched reaction solutions. See Scheme S1 for other possible structures

MDOP monomers by vacuuming promotes the depolymerization from MDOP homosequences at chain ends (Scheme 1E). MDOP depolymerization does not occur when a cyclic ester-derived unit is present at the penultimate position (Scheme 1E, right); however, midchain MDOP homosequences are transferred into chain ends via transacetalization reactions (Scheme 1F), triggering the resumption of MDOP depolymerization. Depolymerization and transacetalization reactions continuously occur until polymer chains with alternating sequences are generated (Scheme 2A). The poorer stability of MDOP homosequences, as suggested by the low  $T_c$  (−37 °C for an equilibrium monomer concentration of 1 M [20]), than the MDOP- $\gamma$ BL heterosequences is likely responsible for the generation of alternating sequences through MDOP depolymerization from its homosequences.

Unlike the copolymerizations that occur with  $\epsilon$ CL [12], when the polymerization mixture was vacuumed, the alternating copolymer degraded into oligomeric products even after the alternating copolymer was generated. After vacuuming was performed for an additional 8 h, a product with an  $M_n$  of  $0.6 \times 10^3$  was obtained (Fig. 3A, (iii)). The  $^1\text{H}$  NMR spectrum of the product exhibited peaks assignable to both MDOP and  $\gamma$ BL units, although MDOP-derived peaks were likely small compared to  $\gamma$ BL-derived peaks (Fig. 3B,

(iii)). The degradation of the alternating copolymer most likely resulted from the depolymerization of  $\gamma$ BL units at the chain end (Scheme 1D), unlike the inertness of the  $\epsilon$ CL units for depolymerization (Scheme 1C) [12]. Removing the “unzipped”  $\gamma$ BL monomers and MDOP monomers from the reaction mixture by vacuuming further promoted the depolymerization reactions (Scheme 2A).

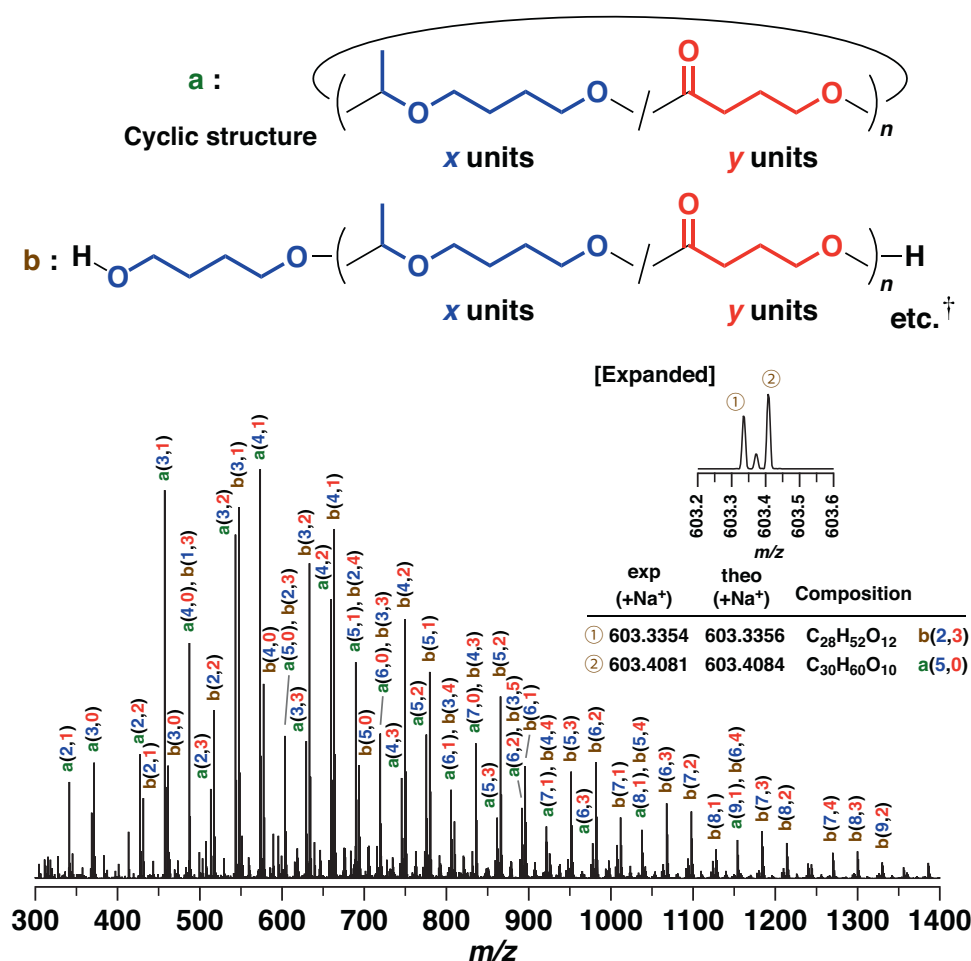
### Reversible control of the polymerization–depolymerization equilibrium by changing the temperature

Another method used to control the polymerization–depolymerization equilibrium is changing the temperature. Unlike irreversible depolymerization in the vacuuming method, which results from the removal of depolymerized monomers from the reaction mixture, the method relying on temperature change is potentially reversible because depolymerized monomers are present in the reaction solution. As shown in our previous study, a copolymer of MDOP and  $\delta$ VL changed into an alternating copolymer upon heating and subsequently returned into a copolymer with MDOP homosequences upon cooling in a reversible manner [13]. Utilizing  $\gamma$ BL instead of  $\delta$ VL should induce degradation to oligomeric products upon



**Fig. 5** ESI-MS spectrum of the product obtained by the copolymerization of MDOP and  $\gamma$ BL after the temperature was increased to 90 °C (see Fig. 4 for the polymerization conditions).

<sup>†</sup>Various structures containing ethylidene or butylenedioxy units are possibly present (see Scheme S1)



heating, as observed with the vacuuming method, and subsequent regeneration of a polymer upon cooling.

To demonstrate the temperature change method, a copolymerization of MDOP and  $\gamma$ BL was first conducted at 30 °C with EtSO<sub>3</sub>H as a catalyst. A product, which was withdrawn from the polymerization solution after 282 h, had an  $M_n$  of  $2.0 \times 10^3$  (Fig. 4A, (i)) and an average number of MDOP/ $\gamma$ BL units per block of 2.5/1.2 (Fig. 4B, (i)). When the temperature was increased to 60 °C, the MW slightly decreased to an  $M_n$  of  $1.5 \times 10^3$  (Fig. 4A, (ii)). The MDOP units per block also decreased from 2.5 to 2.2 (Fig. 4B, (ii)), while the number of  $\gamma$ BL units per block was unchanged (1.2). This result suggests that MDOP monomers were partly removed from MDOP homosequences due to the promotion of depolymerization (Scheme 1E) at high temperature (Scheme 2B).

A further increase in temperature to 90 °C resulted in a drastic decrease in the MW of a product. The higher-MW portion of the MWD peaks observed in the products at 30 and 60 °C disappeared at 90 °C (Fig. 4A, (iii)). The  $M_n$  value of the oligomeric product was  $0.6 \times 10^3$ . The monomer conversion values of MDOP and  $\gamma$ BL were 7% and 3%, which were much lower than the values of 29% and 17%, respectively, at 30 °C. A

relatively large peak assignable to the chain end hydroxy group-adjacent methylene group was observed in the <sup>1</sup>H NMR spectrum of the product (Fig. 4B, (iii)). ESI-MS analysis of the product obtained at this stage revealed that linear and cyclic oligomer chains consisting of MDOP and  $\gamma$ BL units were present (Fig. 5). These results indicate that depolymerization of MDOP and  $\gamma$ BL units (Scheme 1E, D) was highly promoted at this temperature (Scheme 2B).

Importantly, the presence of MDOP and  $\gamma$ BL monomers was confirmed by <sup>1</sup>H NMR analysis of the reaction solution obtained at 90 °C, while undesired side products were not observed (Fig. 4C, (iii)). Therefore, subsequent cooling of the reaction solution at 30 °C led to the regeneration of a polymer product due to the shift in polymerization–depolymerization equilibrium to the polymer side. The monomer conversion values of MDOP and  $\gamma$ BL returned to 31% and 20%, respectively. The polymer exhibited a comparable  $M_n$  value ( $1.7 \times 10^3$ ; Fig. 4A, (iv)) and number of MDOP/ $\gamma$ BL units per block (2.4/1.2; Fig. 4B, (iv)) to those of the polymer obtained before heating. Due to the absence of undesired reactions during the heating–cooling cycle, the polymerization–depolymerization equilibrium was

successfully controlled by changing the temperature (Scheme 2B). It could be possible to depolymerize all polymer and oligomer chains into monomers by combining the heating and vacuuming methods.

## Conclusion

In conclusion, monomer sequence transformation and reversible polymerization–depolymerization control were achieved by vacuuming or changing the temperature in the cationic copolymerization of MDOP and  $\gamma$ BL. The removal of MDOP and  $\gamma$ BL monomers from the polymerization solution with a vacuum pump promoted depolymerization; as a result, the materials were transformed into pseudo-alternating copolymers and oligomers were subsequently formed. Heating the polymerization solution also promoted monomer sequence transformation and oligomer formation, and when the temperature was decreased, polymerization occurred from monomer molecules generated via depolymerization. Copolymer chains that are similar to those obtained before heating were regenerated upon cooling. In these methods, the polymerization–depolymerization equilibrium and transacetalization reactions are responsible for the smooth transformation of copolymer and oligomer products via changes in monomer concentrations or temperature. The strategy devised in this study will help establish copolymerization reactions through which the MW, monomer sequence, and polymerization–depolymerization cycle can be reversibly controlled.

**Acknowledgements** This work was partially supported by JSPS KAKENHI Grant 18K05217.

**Funding** Open access funding provided by Osaka University.

## Compliance with ethical standards

**Conflict of interest** The authors declare no competing interests.

**Publisher's note** Springer Nature remains neutral with regard to jurisdictional claims in published maps and institutional affiliations.

**Open Access** This article is licensed under a Creative Commons Attribution 4.0 International License, which permits use, sharing, adaptation, distribution and reproduction in any medium or format, as long as you give appropriate credit to the original author(s) and the source, provide a link to the Creative Commons licence, and indicate if changes were made. The images or other third party material in this article are included in the article's Creative Commons licence, unless indicated otherwise in a credit line to the material. If material is not included in the article's Creative Commons licence and your intended use is not permitted by statutory regulation or exceeds the permitted use, you will need to obtain permission directly from the copyright holder. To view a copy of this licence, visit <http://creativecommons.org/licenses/by/4.0/>.

## References

- Plummer CM, Li L, Chen Y. Ring-opening polymerization for the goal of chemically recyclable polymers. *Macromolecules*. 2023;56:731–50.
- Liu Y, Lu XB. Emerging trends in closed-loop recycling polymers: monomer design and catalytic bulk depolymerization. *Chem Eur J*. 2023;29:e202203635.
- Jones GR, Wang HS, Parkatzidis K, Whitefield R, Truong NP, Anastasaki A. Reversed controlled polymerization (RCP): depolymerization from well-defined polymers to monomers. *J Am Chem Soc*. 2023;145:9898–915.
- Shi C, Reilly LT, Chen EYX. Hybrid monomer design synergizing property trade-offs in developing polymers for circularity and performance. *Angew Chem Int Ed*. 2023;62:e202301850.
- Yamashita Y, Okada M, Suyama K, Kasahara H. Equilibrium polymerization of 1,3-dioxolane. *Makromol Chem*. 1968;114:146–54.
- Szymanski R. Equilibrium between 1,3-dioxane and its cyclooligomers. *Makromol Chem*. 1991;192:2961–8.
- Kubisa P, Vairon JP. Ring-opening polymerization of cyclic acetals. In: Matyjaszewski K, Möller M, editors. *Polymer science: a comprehensive reference*. Vol. 4.10. Amsterdam: Elsevier BV; 2012.
- Okamoto Y. Cationic ring-opening polymerization of lactones in the presence of alcohol. *Makromol Chem Macromol Symp*. 1991;42/43:117–33.
- Kubisa P, Penczek S. Cationic activated monomer polymerization of heterocyclic monomers. *Prog Polym Sci*. 1999;24:1409–37.
- Endo T, Shibasaki Y, Sanda F. Controlled ring-opening polymerization of cyclic carbonates and lactones by an activated monomer mechanism. *J Polym Sci Part A Polym Chem*. 2002;40:2190–8.
- Penczek S, Pretula J. Activated monomer mechanism (AMM) in cationic ring-opening polymerization. The origin of the AMM and further development in polymerization of cyclic esters. *ACS Macro Lett*. 2021;10:1377–97.
- Higuchi M, Kanazawa A, Aoshima S. Tandem unzipping and scrambling reactions for the synthesis of alternating copolymers by the cationic ring-opening copolymerization of a cyclic acetal and a cyclic ester. *ACS Macro Lett*. 2020;9:77–83.
- Higuchi M, Kanazawa A, Aoshima S. Unzipping and scrambling reaction-induced sequence control of copolymer chains via temperature changes during cationic ring-opening copolymerization of cyclic acetals and cyclic esters. *J Polym Sci*. 2021;59:2730–41.
- Olsen P, Odelius K, Albertsson AC. Thermodynamic presynthetic considerations for ring-opening polymerization. *Biomacromolecules*. 2016;17:699–709.
- Song Q, Zhao J, Zhang G, Peruch F, Carlotti S. Ring-opening (co) polymerization of  $\gamma$ -butyrolactone: a review. *Polym J*. 2020;52:3–11.
- Song Q, Pascouau C, Zhao J, Zhang G, Peruch F, Carlotti S. Ring-opening polymerization of  $\gamma$ -lactones and copolymerization with other cyclic monomers. *Prog Polym Sci*. 2020;110:101309.
- Liu Y, Wu J, Hu X, Zhu N, Guo K. Advances, challenges, and opportunities of poly( $\gamma$ -butyrolactone)-based recyclable polymers. *ACS Macro Lett*. 2021;10:284–96.
- Hong M, Chen EYX. Completely recyclable biopolymers with linear and cyclic topologies via ring-opening polymerization of  $\gamma$ -butyrolactone. *Nat Chem*. 2016;8:42–9.
- Ren C, Li H, Li Y, Liu S, Li Z. Selective ring-opening polymerization of non-strained  $\gamma$ -butyrolactone catalyzed by a cyclic trimeric phosphazene base. *Angew Chem Int Ed*. 2017;56:12987–90.
- Okada M, Yagi K, Sumitomo H. Cationic polymerization of 2-methyl-1,3-dioxepane. *Makromol Chem*. 1973;163:225–34.
- Guthrie JP. Hydrolysis of esters of oxy acids:  $pK_a$  values for strong acids; Brønsted relationship for attack of water at methyl; free energies of hydrolysis of esters of oxy acids; and a linear relationship between free energy of hydrolysis and  $pK_a$  holding over a range of 20 pK units. *Can J Chem*. 1978;56:2342.